Published in final edited form as:
J Steroid Biochem Mol Biol. 2014 September ; 0: 105–114. doi:10.1016/j.jsbmb.2014.01.017.

Differential Effects of Estrogen Exposure on Arylsulfatase B, Galactose-6-Sulfatase, and Steroid Sulfatase in Rat Prostate Development

Leo Feferman, M.D.[1,2], **Sumit Bhattacharyya, Ph.D.**[1,2], **Lynn Birch, M.S.**[3], **Gail S. Prins, Ph.D.**[3], and **Joanne K. Tobacman, M.D.**[1,2]

[1]Department of Medicine, University of Illinois at Chicago, Chicago, IL

[2]Jesse Brown VA Medical Center, Chicago, IL

[3]Department of Urology, University of Illinois at Chicago, Chicago, IL

Abstract

Sulfatase enzymes remove sulfate groups from sulfated steroid hormones, including estrone-sulfate and dehydroepiandrosterone-sulfate, and from sulfated glycosaminoglycans (GAGs), including chondroitin sulfates and heparan sulfate. The enzymes N-acetylgalactosamine-4-sulfatase (Arylsulfatase B; ARSB) and N-acetylgalactosamine-6-sulfatase (GALNS), which remove sulfate groups from the sulfated GAGs chondroitin 4-sulfate (C4S) and chondroitin 6-sulfate, respectively, have not been studied in prostate development previously. In this report, the endogenous variation and the impact of exogenous estradiol benzoate on the immunohistochemistry and activity of ARSB and GALNS in post-natal (days 1–30) ventral rat prostate are presented, as well as measurements of steroid sulfatase activity (STS), C4S, total sulfated GAGs, and versican, an extracellular matrix proteoglycan with chondroitin sulfate attachments on days 5 and 30. Findings demonstrate distinct and reciprocal localization of ARSB and GALNS, with ARSB predominant in the stroma and GALNS predominant in the epithelium. Control ARSB activity increased significantly between days 5 and 30, but following estrogen exposure (estradiol benzoate 25 μg in 25 μl sesame oil subcutaneously on days 1, 3, and 5), activity was reduced and the observed increase on day 30 was inhibited. However, estrogen treatment did not inhibit the increase in GALNS activity between days 5 and 30, and reduced STS activity by 50% on both days 5 and 30 compared to vehicle control. Sulfated GAGs, C4S, and the extracellular matrix proteoglycan versican declined between days 5 and 30 in the control, but these declines were inhibited following estrogen. Study findings indicate distinct variation in expression and activity of sulfatases, sulfated GAGs, C4S, and versican in the process of normal prostate development, and disruption of these events by exogenous estrogen.

Address correspondence to: Joanne K. Tobacman, M.D., Department of Medicine, University of Illinois at Chicago, 840 S. Wood St., CSN 440, M/C 718, Chicago, IL 60612, Telephone: 312-569-7826, Fax: 312-413-8283, jkt@uic.edu.

Keywords

estradiol; steroid sulfatase; chondroitin sulfate; versican; glycosaminoglycans; sulfatase

Introduction

Sulfatase enzymes comprise a group of cellular and extracellular enzymes that are key regulators of the degradation of sulfated glycosaminoglycans, including chondroitin sulfate, dermatan sulfate, keratan sulfate, heparin, and heparan sulfate, and of sulfated steroids, including estrone sulfate and dehydroepiandrosterone sulfate. Arylsulfatase B (ARSB; N-acetylgalactosamine-4-sulfatase) and N-acetylgalactosamine-6-sulfatase (GALNS) are enzymes that remove sulfate groups from the sulfated glycosaminoglycans (GAGs) chondroitin 4-sulfate (C4S) and chondroitin 6-sulfate (C6S), respectively. Deficiency of ARSB or GALNS leads to accumulation of sulfated glycosaminoglycans, resulting in the lysosomal storage diseases Mucopolysaccharidosis (MPS) VI from ARSB deficiency and MPS IVA from GALNS deficiency. Removal of the 4-sulfate group is required for the degradation of C4S, and removal of the sulfate group is required for activity of steroid hormones. Prior experiments in human mammary cell lines demonstrated that 1) estrone (100 pg/ml) and estradiol (200 pg/ml) exposure significantly reduced activity of steroid sulfatase (STS) and ARSB, but not of GALNS in MCF-7 and T47D cells; and 2) GALNS activity was significantly higher in primary mammary epithelial cells, whereas ARSB and STS activity were higher in primary myoepithelial cells [1]. In this report, we present *in vivo* data that expand on these prior *in vitro* observations of sulfatase activity and response to exogenous estrogen and report the endogenous sulfatase activity and expression and the impact of estrogen exposure on sulfatase activity in a rodent model of prostate development.

This study, by elucidating differences between activity and distribution of sulfatases in both the native prostate and following estrogen treatment, presents a novel approach to prostate morphogenesis, focusing on activity and expression of sulfatases that modify chondroitin sulfate and on the associated changes in total sulfated GAGs, C4S, and the ECM proteoglycan versican. Decline in ARSB activity has been shown in malignant prostate tissue, malignant colon tissue, malignant mammary cells, and metastatic colonic cell lines [1, 2–6]. In human prostate cells, decline in ARSB produced increases in total sulfated GAGs, C4S, and versican [2, 3]. Previously, both versican and chondroitin sulfate have been identified as biomarkers of more aggressive prostate cancer [7, 8]. Versican is a large, aggregating extracellular matrix proteoglycan with chondroitin sulfate attachments that interacts with multiple cell surface receptors and recruits signaling molecules to the cell surface, thus modulating signaling pathways and stromal-epithelial interactions [3, 9–11].

The profiles of ARSB, GALNS, and STS enzyme activity and localization and of total sulfated GAGs, C4S and versican in the developing rat prostate have not previously been addressed. In the rodent, prostate development occurs predominantly in early post-natal life, and high doses of exogenous natural estrogens caused developmental and differentiation defects in the adult prostate [12]. In this report, measurements of ARSB, GALNS, and steroid sulfatase (STS) activity, total sulfated GAGs, C4S, and the proteoglycan versican on

days 5 and 30 of post-natal development in rat prostate tissue are presented. The impact of an intermediate dose of exogenous estradiol benzoate (25 μg) exposure on days 1,3, and 5 of post-natal life on these parameters and on ARSB and GALNS immunohistochemistry on post-natal days 1, 3, 6, 10, 15, and 30 is presented. Since decline in ARSB activity has been associated with prostate neoplasia [2, 3], insight into the interactions among estrogen, ARSB, GALNS, and STS in prostate development may lead to better understanding of the effects of steroid hormones on stromal-epithelial interactions and on mechanisms of prostate carcinogenesis.

Methods

Animal Care and Treatment

All procedures were approved by the Institutional Animal Care and Use Committee (IACUC) of the University of Illinois at Chicago. 96 male Sprague-Dawley rats (Zivic-Miller, Pittsburgh, PA) were treated with subcutaneous injections of either 25 μl sesame oil alone (controls) or high-dose estrogen (25 ug estradiol benzoate in 25 μl sesame oil) on post-natal days 1, 3, and 5 as previously described [12, 13]. Twelve animals (6 control and 6 estrogen-treated) were euthanized on days 1, 3, 6, 10, 15, and 30, and the prostates were removed, formalin-fixed, paraffin-embedded and sectioned, as previously detailed [14–17]. In addition, prostate tissue from similarly estrogen-treated and vehicle control animals was obtained from rats sacrificed on day 5 (total n=12) and on day 30 (total n=12).

ARSB and GALNS immunohistochemistry

Sections of the estrogen-treated and control ventral prostate tissues were mounted on the same slide and immunostained. Antigen retrieval was done with pH 6.1 citrate buffer at 90°C for 40 minutes. For ARSB, the slides were incubated overnight with rabbit polyclonal antibody (1:50; Open Biosystems, Huntsville, AL), then for 1 hour with anti-rabbit IgG-HRP at 1:1000 dilution. Color was developed with 3,3'-Diaminobenzidine (DAB) for 5 minutes. For GALNS, slides were incubated overnight with rabbit polyclonal antibody (1:200; Open Biosystems, Huntsville, AL), followed by anti-rabbit IgG-HRP at 1:1000 dilution for 1 hour and DAB for 5 minutes and counterstained with hematoxylin. The sections were blocked with a serum-free Universal Blocking Solution from Biocare Medical (Concord, CA). Negative control used normal rabbit IgG diluted in buffer at the same dilution as used for the primary antibody (1:50 for ARSB; 1:200 for GALNS), and all other staining procedures were similar. Positive controls were sections of adult human prostate. Digitized images were obtained with QCapture software (QImaging, Surrey, BC, Canada) at 20X magnification. Background and brightness were modified with GIMP Portable software (Portable Apps, New York, NY) or with Adobe Photoshop (CS2). Qualitative assessments of intensity and distribution of ARSB and GALNS immunostaining were made by three study investigators (LF, GSP, JKT), who agreed on the descriptive findings that are reported.

Determination of ARSB, GALNS, and STS activity in prostate tissue homogenates

Homogenates were prepared from ventral prostate tissue of estrogen-treated and control rats on days 5 and day 30 of post-natal development (total n=24). Arylsulfatase B (ARSB; N-

acetylgalactosamine-4-sulfatase) activity measurements were performed using a fluorometric assay, as previously, with 20 μl of tissue homogenate, 80 μl of assay buffer (0.05 M Na acetate buffer, pH 5.6), and 100 μl of substrate [5mM 4-methylumbelliferyl sulfate (MUS) in assay buffer] in wells of a microplate [1, 18, 19]. The microplate was incubated for 30 minutes at 37°C, and the reaction was stopped by 150 μl of stop buffer (Glycine-Carbonate buffer, pH 10.7), and fluorescence was measured at 360 nm (excitation) and 465 nm (emission) in a microplate reader (FLUOstar, BMG, Cary, North Carolina). Activity was expressed as nmol/mg protein/hour, based on a standard curve for ARSB activity prepared with known quantities of 4-methylumbelliferyl at pH 5.6. Protein was determined by total protein assay kit (Pierce, Thermo Fisher Scientific, Inc., Rockford, IL).

For STS determination, six 20 μl prostate tissue homogenates were incubated with 80 μl of assay buffer (0.5M Tris-Cl Buffer, pH 7.5), and 100 μl of substrate (0.5 mM 4-MUS in assay buffer), as previously detailed [1, 18, 20]. The reaction mixture was incubated for 4 hours at 37°C, at which time 100 μl of stop buffer (1M Tris-Cl buffer at pH 10.4) was added, and fluorescence was measured in a microplate reader (BMG). Activity was expressed as nmol/mg protein/h, and was derived from a standard curve prepared with known quantities of 4-methylumbelliferyl at pH 7.5. Protein was determined by total protein assay kit (Pierce).

The measurement of Galactose-6-sulfatase (GALNS) activity was performed using 5 μl of tissue homogenate made in ddH_2O by sonication with metal tip, combined with 5 μl 0.2% heat-inactivated BSA (or 10 μl of 0.2% heat-inactivated BSA for blank) and 20 μl of substrate [10 mM 4-methylumbelliferyl-β-D-galactoside-6-sulfateNH_4 (MU-βGal-6S)] in substrate buffer (0.1M sodium acetate / 0.1M acetic acid at pH 4.3 with 0.1M NaCl, 5mM Pb-acetate (1.9 mg/ml) and 0.02% Na-azide) in wells of a microplate [1, 18, 21]. After incubation for 17 hours at 37°C, 5μl 0.9 M Na-Phosphate buffer at pH 4.3 with 0.02% Na-azide was added, as well as 10μl of 10 U β-D-Galactoside galactohydrolase (Sigma) / ml 0.2% heat-inactivated BSA. After incubation for 2 hours at 37°C, 200 μl of stop buffer (0.5M $NaHCO_3$ / 0.5M Na_2CO_3 at pH 10.7 with 0.025% Triton-X-100) was added, and readings of fluorescence were taken at 360 nm and 465 nm in a plate reader (BMG). GALNS activity was expressed as nmol/mg protein/h, and protein was determined by total protein assay kit (Pierce).

Measurement of total sulfated glycosaminoglycans

Total sulfated glycosaminoglycans (GAG) in control and estrogen-treated rat prostate tissue were measured using 1,9-dimethylmethylene blue (Blyscan™, Biocolor Ltd., Newtownabbey, Northern Ireland), as previously detailed [5, 22]. The sulfated polysaccharide component of proteoglycans (PG) and protein-free sulfated GAG chains were detected, whereas disaccharides and hyaluronan were not detected. The reaction was performed in the presence of excess unbound dye. The cationic dye and sGAG at acid pH produced an insoluble dye-GAG complex, and the GAG content was determined by the amount of dye that was recovered from the test sample following exposure to Blyscan dissociation reagent. Absorbance maximum of 1,9-dimethylmethylene blue is 656 nm; sulfated GAG concentration was expressed as μg / mg protein of tissue extract.

Immunoprecipitation of tissue lysates by chondroitin 4-sulfate antibody

Tissue lysates were prepared using RIPA buffer (50 mmol/l Tris-HCl containing 0.15 mol/l NaCl, 1% Nonidet P40, 0.5% deoxycholic acid and 0.1% SDS, pH 7.4). Antibody specific to native C4S (4D1, Abnova, Littleton, CO) was added to lysates in tubes at a concentration of 1 μg/mg of tissue protein, and tubes were rotated overnight in a shaker at 4°C. Next, 100 μl of pre-washed Protein L-Agarose (SCBT, Santa Cruz, CA) was added to each tube, tubes were incubated overnight at 4°C, and the Protein L-Agarose treated beads were washed three times with PBS containing Protease Inhibitor Cocktail, as previously [2, 4]. The precipitate was eluted with dye-free elution buffer and subjected to sulfated GAG assay.

Determination of versican by competitive ELISA

Versican was measured by competitive ELISA (My BioSource, San Diego, CA), in which color development was inversely proportional to the versican content in the test samples. Standards ranging from 1 to 25 ng/ml, samples, and versican-horseradish peroxidase conjugate were added to wells pre-coated with versican antibody, incubated for 1 hour at 37°C, and washed three times. Color was developed by adding hydrogen peroxide / tetramethylbenzidine (TMB) substrate, the reaction was stopped by 2N H_2SO_4, and the color intensity was read at 450 nm in a plate reader (BMG). The concentration of versican in the samples was extrapolated from the standard curve and expressed per mg of total tissue protein, measured by protein assay (Pierce).

Statistics

Unless stated otherwise, one-way ANOVA with Tukey-Kramer post-test was performed using InStat (GraphPad Software, Inc., La Jolla, CA), to compare the measurements between day 5 and day 30 samples and between oil-control and estrogen-treated samples. Six independent tissue samples were analyzed for each time point and for treated and control conditions. Measurements are presented as mean values ± standard deviation (S.D.). P-value of less than 0.05 is considered statistically significant, and * represents $p \leq 0.05$, ** represents $p \leq 0.01$, and ***represents $p \leq 0.001$.

Results

Changes in sulfatase activity, total sulfated glycosaminoglycans, chondroitin-4-sulfate and versican between day 5 and day 30

In the control, oil-treated, rat ventral prostate tissue, the ARSB activity and the GALNS activity both increased significantly between day 5 and day 30, ($p<0.001$, 1-way ANOVA with Tukey-Kramer post-test, n=6 in each group) (Table 1; Fig. 1A, 1B). In contrast, the steroid sulfatase (STS) activity was similar at both time points (Fig. 1C). In association with the increases in ARSB and GALNS, the total sulfated glycosaminoglycans (GAGs) and the chondroitin-4-sulfate (C4S) both declined significantly ($p<0.001$, $p<0.001$) (Fig. 2A, 2B). The extracellular matrix proteoglycan versican, which has chondroitin sulfate attachments, also declined significantly between days 5 and 30, corresponding to the decline in sGAG and C4S (Fig. 2C) ($p<0.001$).

Impact of estrogen exposure on sulfatase activity, total sulfated glycosaminoglycans, chondroitin-4-sulfate, and versican

Following treatment with estradiol benzoate (25 μg / 25 μl sesame oil) on days 1, 3, and 5, the ARSB activity in the prostate tissue was ~14% less on day 5 ($p<0.05$) in the estrogen-treated than in the control tissue (Fig. 1A; Table 1). On day 30, ARSB activity was similar to the day 5 level in the estrogen-treated tissue, but was ~35% less than in the control tissue ($p<0.001$). In contrast, the increase in GALNS activity between days 5 and 30 that occurred in the control tissue also occurred following estrogen, and the day 30 GALNS activity was ~12% higher following estrogen than in the control tissue ($p<0.01$) (Fig. 1B). Following estrogen, steroid sulfatase (STS) activity declined to ~50% of the control level on both days 5 and 30 ($p<0.001$) (Fig. 1C), and was similar at both time points.

ARSB is the enzyme which regulates chondroitin-4-sulfate degradation, so a decline in ARSB activity is anticipated to be associated with increased total sGAG and C4S. Hence, following estrogen exposure and decline in ARSB activity, the normal maturation-associated declines in total sGAG and in C4S between day 5 and day 30 did not occur ($p<0.001$, $p<0.001$) (Fig. 2A, 2B). Levels of total sGAG and C4S were similar on days 5 and 30 following estrogen exposure suggesting that the maximum effect was achieved by day 5. The increase in C4S accounted for ~45% of the total increase in sGAG. In a similar manner, the content of versican in the estrogen-exposed ventral prostate tissue did not decline with maturation between days 5 to day 30. While the versican level in the estrogen exposed ventral lobe on day 5 was the same as levels in the control animal, it was 35% greater than the control value on day 30 ($p<0.001$).

Predominant localization of ARSB in stroma and of GALNS in prostate epithelium

The prostate arises in the urogenital sinus from solid epithelial cords, which are canalized in a proximal to distal direction, beginning on day 1 in the rat ventral prostate. Images of rat ventral prostate on days 1, 3, 6, 10, 15, and 30 present the evolving distinct localization of ARSB (brown) in the stroma and in the luminal membrane of the epithelial cells (Figs. 3A-3F). Reciprocally, GALNS appears more prominent in the developing nests of epithelium (Days 1, 3, 6, and 10), which are negative for ARSB on days 3 and 6 (Figure 3B,C) and positive for GALNS (brown in Figure 4A-4F). ARSB continues to be prominent in the stroma throughout days 1–30, whereas the GALNS staining in the stroma declines, with increased localization in the developing acinar epithelium. An overall increase in intensity and distribution of ARSB is evident between the early and late control images, consistent with the rise in ARSB activity between days 5 and 30 in the control tissue. Similarly, the epithelial GALNS staining intensity appears increased in the Day 30 images, consistent with increased GALNS activity.

Decline in ARSB positive immunostaining with delay in acinar development following exogenous estrogen

Prostate development following estrogen exposure (estradiol benzoate 25 μg on days 1, 3, and 5) is presented in Figs. 5A-5F and 6A-6F. Delay in acinar development post estrogen exposure appears at 15 days (Fig. 5E vs. Fig. 3E) with ARSB immunostaining on day 30 (Fig. 5F) post estrogen resembling vehicle control on day 15 (Fig. 3E). With GALNS

immunostaining, the lumen and acinar structures on day 15 without estrogen (Fig. 4E) appear more advanced than on day 15 following estrogen exposure (Fig. 6E). In the estrogen-treated ventral prostates, the stromal compartment has relatively reduced immunostaining for ARSB, evident on all days 1–30 (Fig. 5A-5F), compared to the day-matched vehicle control (Fig. 3A-3F), and consistent with the measured decline in ARSB activity between days 5 and 30. Negative ARSB immunostaining of epithelium is best seen in control on day 3 (Fig. 3B) and in estrogen-treated on day 6 (Fig. 5C), consistent with a developmental delay. Luminal membrane appears positive for both ARSB and GALNS on day 30 (Figs. 5F6F). These findings suggest that the decline in stromal ARSB delays the development of the acinar structures, indicating impaired stromal-epithelial interaction following exogenous estrogen.

Discussion

This study presents new information about activity and expression of sulfatases in rat prostate development, and the impact of estrogen exposure on sulfatase activity, as well as on content of total sulfated glycosaminoglycans, chondroitin-4-sulfate, and the extracellular matrix proteoglycan versican. In the normal developing rat ventral prostate, ARSB activity and GALNS activity increased between days 5 and 30, with an associated decline in the total sulfated GAGs, C4S, and versican. In contrast, steroid sulfatase activity was similar at these two time points. Following exposure to estradiol benzoate (25 μg subcutaneous injection on days 1, 3, and 5), ARSB activity was 14% less than vehicle control on day 5 and 35% less than vehicle control on day 30. In contrast, GALNS activity increased in both control and estrogen-treated tissue between days 5 and 30, and was slightly higher in the estrogen-treated tissue. Steroid sulfatase activity was reduced by ~50% following estrogen treatment at both time points. Total sulfated GAGs, C4S, and the extracellular matrix proteoglycan versican were significantly increased at 30 days, compared to vehicle controls. Hence, neonatal exposure to this dose and preparation of estrogen inhibited the normal increase in ARSB, suppressed STS, and increased C4S, total sulfated GAGs, and versican. These responses suggest that some of the mechanisms by which estrogen produces its effects in prostatic tissue may be mediated through changes in sulfatases and chondroitin sulfate.

Since estrogen receptor alpha (ERα) is present in the stromal tissue of the developing prostate [23, 24], but not in the epithelial cells, the decline in ARSB is consistent with a response to estrogen in the stromal cells where ARSB predominates, as shown by immunostaining. In contrast, the increase in GALNS is not inhibited by estrogen, since the epithelial cells, where GALNS immunostaining predominates, does not have ERs. The reciprocal localization of ARSB and GALNS immunostaining seen in the developing rat ventral prostate indicates that these sulfatase enzymes may have an impact upon the interaction between stromal and epithelial compartments in prostate morphogenesis. Disruption of their normal coordinated increases by estrogen may contribute to disordered development of the prostate. Disruption of normal prostate development can lead to irreversible morphogenic defects which affect the function of the prostate throughout life, as evidenced by the impact of aberrant estrogenic exposures during early development, predisposing the prostate to chronic inflammation and neoplasia with aging [13, 16, 25].

The dose of estradiol used in the studies of this report is intermediate in the range of estradiol benzoate previously tested, which included 0.015 ug/kg body weight to 15 mg/kg body weight [26]. Changes in body weight or in relative weight of the ventral prostate lobe (ventral lobe in mg/ 100 mg body weight) did not vary in a dose-dependent manner when the rats were euthanized on day 35 or day 90, following subcutaneous injections on days 1, 3, and 5. No significant change in the relative weight of the ventral prostate lobe was evident with an estradiol benzoate (EB) dose of 150 ug/kg body weight on days 1, 3, and 5, which is comparable to the EB dose used in the current studies (25 μg / ~160 g body weight). Body weight was significantly reduced on day 35 (183.8 ± 5.59 g for vehicle control vs. 161.6 ± 7.2 g for EB dose of 150 μg/kg body weight, n=8 for each group; $p<0.001$) or on day 90 following EB, compared to vehicle control. At the low dose (0.15 μg/kg body weight), EB did not modify the presence or localization of androgen receptors, the number of basal cells, the number of differentiated luminal cells, or the characteristics of periacinar and perivascular smooth muscle cells. However, increasing concentrations of EB caused progressive decline in the number of androgen receptor positive cells, increasing numbers of basal cells, decline in luminal epithelial cells, and increased extension of the multilayered fibroblast sheath into the distal tips of the prostatic ducts, so that smooth muscle cells were no longer in contact with the epithelium [26].

Prostate gland development involves significant remodeling of tissue architecture that includes reorganization of stromal and epithelial cells, basement membranes and extracellular matrices (ECM) [12]. Neonatal estrogen exposure perturbs the normal stromal-epithelial development [14, 16, 25–28], such as suggested by the changes in sulfatases, sulfated GAGs, and versican in our studies. Following neonatal estrogen exposure in this study, the ARSB immunostaining in the stroma was less intense. When ARSB was reduced following estrogen exposure, C4S and sGAG increased, due to decline in their normal degradation which requires ARSB. The increases in total sGAG and C4S in the prostate tissue when ARSB was reduced may contribute to impaired morphogenesis, due to inhibition of the normal stromal-epithelial signaling of chemokines and growth factors by the increased sGAG content [29–31]. The mechanism by which estrogen exposure leads to reduced ARSB is unknown at this time, and the extent to which decline in ARSB (with the associated increase in C4S) and in STS activity contributes to the overall impact of estrogen on the prostate is not yet discernible. The decline in versican, however, is likely attributable to a transcriptional mechanism which follows from the decline in ARSB and the associated increase in chondroitin-4-sulfation. Galectin-3, a β-galactoside-associated lectin, binds less to more highly sulfated C4S when ARSB is reduced, and is more abundant in the nucleus, where it activates the versican promoter in association with AP-1 components c-jun and c-fos [3, 32].

The effects of ARSB and of GALNS in prostate development have not been reported previously, although changes in chondroitin sulfates (CS) and in versican have been studied in prostate development [33, 34]. When guinea pigs were given estradiol, the CS was increased compared with the post-pubertal level, similar to the present findings in the estrogen-treated neonatal rat prostate. In contrast, when circulating dihydrotestosterone increased at puberty, periglandular and fibromuscular stromal staining intensity for native total chondroitin sulfate (immunostained with CS56 antibody) decreased 11-fold in the

guinea pig prostate. Similarly, chondroitin sulfate declined in castrated guinea pigs given DHT replacement. Sakko *et al* hypothesized that both chondroitin sulfate and versican expression were negatively regulated by androgen, and showed that versican in the periacinar fibromuscular stroma peripheral to the basal epithelial cells as well as in loose fibrovascular connective tissue between acini decreased during normal pubertal development in association with increased circulating levels of androgen [34].

Other proteoglycans, including small-leucine rich proteoglycans (decorin, biglycan, and lumican), syndecan-1, betaglycan, and perlecan are also present in the prostate [35]. The GAG attachments of the proteoglycans affect the binding of ligands, including fibroblast growth factor (FGF)2 and FGF10, which bind to heparan sulfate (HS). Perlecan, which has both chondroitin sulfate and heparan sulfate attachments, has been proposed as a likely candidate for the HS proteoglycan that is active during prostate development [35]. Other sulfatases, including iduronate 2-sulfatase and Sulf1, have been identified in prostate tissue. The enzyme iduronate 2-sulfatase, which removes 2-sulfate groups from iduronate residues of HS or heparin, was one of 13 genes overexpressed in 16-month-old rat ventral prostate tissue compared with three-month-old rat tissue, suggesting a role in aging prostate tissue [36]. In cultured urogenital sinus (UGS) tissues from mouse embryos at different stages of development, expression of Sulfatase 1 (Sulf1), the enzyme that catalyses the hydrolysis of 6-O sulfates from heparan sulfate, was significantly decreased in male compared to female UGS as development progressed [37, 38]. This decrease was correlated with morphological changes in prostatic epithelial bud outgrowth, and interruption of HS 6-sulfation by ectopic expression of Sulf1 partially inhibited the testosterone-induced ductal morphogenesis and impaired FGF10 signaling. This further supports the present data and indicates a specific role for multiple sulfatases in tissue remodeling necessary for the development of normal prostate gland architecture.

Future work will be designed to integrate the findings in the current report to other observations about the programmed development of the prostate and the role of sulfatases, GAGs, and proteoglycans. Further evaluation of the interrelationships among ARSB, GALNS, C4S, C6S, and versican with estrogens and testosterone are anticipated to provide new insights into stromal-epithelial interactions in the developing prostate and into the mechanisms that affect cell fate determinations in prostate carcinogenesis.

Conclusions

Study findings demonstrate significant differences between the localization and the response to estrogen of the chondroitin sulfate modifying enzymes ARSB and GALNS in the developing ventral rat prostate. Immunohistochemistry demonstrated predominance of ARSB in the cytoplasm of the stroma and of GALNS in the cytoplasm of the epithelium. Between days 5 and 30, in the vehicle-only controls, ARSB activity increased, GALNS activity increased, STS did not change, and total sulfated GAGs, C4S, and versican declined. Following estrogen exposure, ARSB activity declined significantly, GALNS increased slightly, STS declined by almost 50%, and total sulfated GAGs, C4S, and versican all increased significantly. These results indicate that ARSB and GALNS are important in the development of the normal prostate architecture, and that some of the mechanisms by

which estrogen produces its effects in the prostate may be mediated through changes in sulfatases and chondroitin sulfates.

Acknowledgments

Funding sources include DK40890 to GP and ULI RR029879 pilot grant to JKT.

References

1. Bhattacharyya S, Tobacman JK. Steroid sulfatase, arylsulfatases A and B galactose 6-sulfatase, and iduronate sulfatase in mammary cells and effects of sulfated and non-sulfated estrogens on sulfatase activity. J. Steroid Biochem Mol Biol. 2007; 103(1):20–34. [PubMed: 17064891]
2. Feferman L, Bhattacharyya S, Deaton R, Gann P, Guzman G, Kajdacsy-Balla A, Tobacman JK. Arylsulfatase B (N-acetylgalactosamine-4-sulfatase): potential role as a biomarker in prostate cancer. Prostate Cancer Prostatic Dis. 2013 Jul 9. [Epub ahead of print].
3. Bhattacharyya S, Feferman L, Tobacman JK. Galectin-3 and AP-1 mediate transcriptional effect of Arylsulfatase B (N-acetylgalactosamine-4-sulfatase) on versican in prostate cancer. Oncogene. 2013 [Epub ahead of print].
4. Prabhu SV, Bhattacharyya S, Guzman-Hartman G, Macias V, Kajdacsy-Balla A, Tobacman JK. Extra-lysosomal localization of arylsulfatase B in human colonic epithelium. J Histochem Cytochem. 2011; 59(3):328–335. [PubMed: 21378286]
5. Bhattacharyya S, Kotlo K, Shukla S, Danziger RS, Tobacman JK. Distinct effects of N-acetylgalactosamine-4-sulfatase and galactose-6-sulfatase expression on chondroitin sulfate. J Biol Chem. 2008; 283(15):9523–9530. [PubMed: 18285341]
6. Bhattacharyya S, Tobacman JK. Arylsulfatase B regulates colonic epithelial cell migration by effects on MMP9 expression and RhoA activation. Clin Exp Metastasis. 2009; 26(6):535–545. [PubMed: 19306108]
7. Ricciardelli C, Mayne K, Sykes PJ, Raymond WA, McCaul K, Marshall VR, Tilley WD, Skinner JM, Horsfall DJ. Elevated stromal chondroitin sulfate glycosaminoglycan predicts progression in early-stage prostate cancer. Clin Cancer Res. 1997; 3:983–992. [PubMed: 9815775]
8. Ricciardelli C, Mayne K, Sykes PJ, Raymond WA, McCaul K, Marshall VR, Horsfall DJ. Elevated levels of versican but not decorin predict disease progression in early-stage prostate cancer. Clin Cancer Res. 1998; 4:963–971. [PubMed: 9563891]
9. Sakko AJ, Ricciardelli C, Mayne K, Suwiwat S, LeBaron RG, Marshall VR, Tilley WD, Horsfall DJ. Modulation of prostate cancer cell attachment to matrix by versican. Cancer Res. 2003; 63:4786–4791. [PubMed: 12941795]
10. Kischel P, Waltregny D, Dumont B, Turtoi A, Greffe Y, Kirsch S, De Pauw E, Castronovo V. Versican overexpression in human breast cancer lesions: known and new isoforms for stromal tumor targeting. Int J Cancer. 2010; 126:640–650. [PubMed: 19662655]
11. Ricciardelli C, Sakko AJ, Ween MP, Russell DL, Horsfall DJ. The biological role and regulation of versican levels in cancer. Cancer Metastasis Rev. 2009; 28:233–245. [PubMed: 19160015]
12. Prins GS, Putz O. Molecular signaling pathways that regulate prostate gland development. Differentiation. 2008; 76:641–659. [PubMed: 18462433]
13. Prins GS. Neonatal estrogen exposure induces lobe-specific alterations in adult rat prostate androgen receptor expression. Endocrinology. 1992; 130:3703–3714. [PubMed: 1597166]
14. Prins GS, Birch L. The developmental pattern of androgen receptor expression in rat prostate lobes is altered after neonatal exposure to estrogen. Endocrinology. 1995; 136:1303–1314. [PubMed: 7867585]
15. Prins GS, Birch L. Neonatal estrogen exposure up-regulates estrogen receptor expression in the developing and adult rat prostate lobes. Endocrinology. 1997; 138:1801–1809. [PubMed: 9112371]

16. Chang WY, Wilson MJ, Birch L, Prins GS. Neonatal estrogen stimulates proliferation of periductal fibroblasts and alters the extracellular matrix composition in the rat prostate. Endocrinology. 1999; 140:405–415. [PubMed: 9886852]
17. Cunha GR, Ricke W, Thomson A, Marker PC, Risbridger G, Hayward SW, Wang YZ, Donjacour AA, Kurita T. Hormonal, cellular, and molecular regulation of normal and neoplastic prostatic development. J Steroid Biochem Mol Biol. 2004; 92(4):221–236. [PubMed: 15663986]
18. Bhattacharyya S, Look D, Tobacman JK. Increased arylsulfatase B activity in cystic fibrosis cells following correction of CFTR. Clin Chim Acta. 2007; 380(1–2):122–127. [PubMed: 17324393]
19. Roy AB. Arylsulfatases, colorimetric and fluorimetric assays. Methods Enzymol. 1987; 143:207–217. [PubMed: 3657536]
20. Wolff B, Billich A, Brunowsky W, Herzig G, Lindley I, Nussbaumer P, Pursch E, Rabeck C, Winkler G. Microtiter plate cellular assay for human steroid sulfatase with fluorescence readout. Anal Biochem. 2003; 318:276–284. [PubMed: 12814632]
21. van Diggelen OP, Zhao H, Kleijer WJ, Janse BJHM, Poorthuis J, van Pelt J, Kamerling JP, Glajaard H. A fluorimetric enzyme assay for the diagnosis of Morquio disease type A. Clin Chim Acta. 1990; 187:131–140. [PubMed: 2107987]
22. Blyscan™ Sulfated GAG Assay. Bio.Bly.VER.03-12March2012int. www.biocolor.co.uk
23. Prins GS, Birch L. Neonatal estrogen exposure up-regulates estrogen receptor expression in the developing and adult rat prostate lobes. Endocrinology. 1997; 138(5):1801–1809. [PubMed: 9112371]
24. Prins GS, Birch L, Couse JF, Choi I, Katzenellenbogen B, Korach KS. Estrogen imprinting of the developing prostate gland is mediated through stromal estrogen receptor alpha: studies with alphaERKO and betaERKO mice. Cancer Res. 2001; 61(16):6089–6097. [PubMed: 11507058]
25. Prins GS, Birch L, Tang WY, Ho SM. Developmental estrogen exposures predispose to prostate carcinogenesis with aging. Reprod Toxicol. 2007; 23(3):374–382. [PubMed: 17123779]
26. Putz O, Schwartz CB, Kim S, LeBlanc GA, Cooper RL, Prins GS. Neonatal low- and high-dose exposure to estradiol benzoate in the male rat: I Effects on the prostate gland. Biol Reprod. 2001; 65:1496–1505. [PubMed: 11673267]
27. Chang WY, Birch L, Woodham C, Gold L, Prins GS. Neonatal estrogen exposure alters the TGFβ signaling system in the developing rat prostate and interrupts TGFβ-mediated differentiation of the epithelium. Endocrinology. 1999; 140:2801–2813. [PubMed: 10342871]
28. Habermann H, Chang WY, Birch L, Mehta P, Prins GS. Developmental exposure to estrogens alters epithelial cell adhesion and gap junction proteins in the adult rat prostate. Endocrinology. 2001; 142:359–369. [PubMed: 11145599]
29. Frevert CW, Kinsella MG, Vathanaprida C, Goodman RB, Baskin DG, Proudfoot A, Wells TN, Wight TN, Martin TR. Binding of interleukin-8 to heparan sulfate and chondroitin sulfate in lung tissue. Am J Respir Cell Mol Biol. 2003; 28:464–472. [PubMed: 12654635]
30. Kuschert GS, Coulin F, Power CA, Proudfoot AE, Hubbard RE, Hoogewerf AJ, Wells TN. Glycosaminoglycans interact selectively with chemokines and modulate receptor binding and cellular responses. Biochemistry. 1999; 38:12959–12968. [PubMed: 10504268]
31. Handel TM, Johnson Z, Crown SE, Lau EK, Proudfoot AE. Regulation of protein function by glycosaminoglycans - as exemplified by chemokines. Annu Rev Biochem. 2005; 74:385–410. [PubMed: 15952892]
32. Bhattacharyya S, Tobacman JK. Hypoxia reduces arylsulfatase B activity and silencing arylsulfatase B replicates and mediates the effects of hypoxia. PLoS One. 2012; 7(3):e33250. [PubMed: 22428001]
33. Horsfall DJ, Mayne K, Skinner JM, Saccone GT, Marshall VR, Tilley WD. Glycosaminoglycans of guinea pig prostate fibromuscular stroma: Influence of estrogen and androgen on levels and location of chondroitin sulfate. Prostate. 1994; 25:320–332. [PubMed: 7997436]
34. Sakko AJ, Ricciardelli C, Mayne K, Dours-Zimmermann MT, Zimmermann DR, Neufing P, Tilley WD, Marshall VR, Horsfall DJ. Changes in steroid receptors and proteoglycan expression in the guinea pig prostate stroma during puberty and hormone manipulation. Prostate. 2007; 67:288–300. [PubMed: 17192879]

35. Edwards IJ. Proteoglycans in prostate cancer. Nat Rev Urol. 2012; 9:196–206. [PubMed: 22349653]

36. Lau KM, Tam NN, Thompson C, Cheng RY, Leung YK, Ho SM. Age-associated changes in histology and gene-expression profile in the rat ventral prostate. Lab Invest. 2003; 83:743–757. [PubMed: 12746483]

37. Buresh-Stiemke RA, Malinowski RL, Keil KP, Vezina CM, Oosterhof A, Van Kuppevelt TH, Marker PC. Distinct expression patterns of Sullf1 and Hs6st1 spatially regulate heparan sulfate sulfation during prostate development. Dev Dyn. 2012; 241(12):2005–2013. [PubMed: 23074159]

38. Buresh RA, Kuslak SL, Rusch MA, Vezina CM, Selleck SB, Marker PC. Sulfatase 1 is an inhibitor of ductal morphogenesis with sexually dimorphic expression in the urogenital sinus. Endocrinology. 2010; 151(7):3420–3431. [PubMed: 20410206]

Highlights

- Developing rat prostate has distinct and reciprocal localization of sulfatases
- Arylsulfatase B predominates in stroma, and galactose-6-sulfatase in epithelium
- Arylsulfatase B (ARSB) and galactose-6-sulfatase (GALNS) increased from d5 to
- Increase of ARSB, but not of GALNS, was inhibited by estrogen
- Exogenous high-dose estrogen inhibited steroid sulfatase on d5 and d30

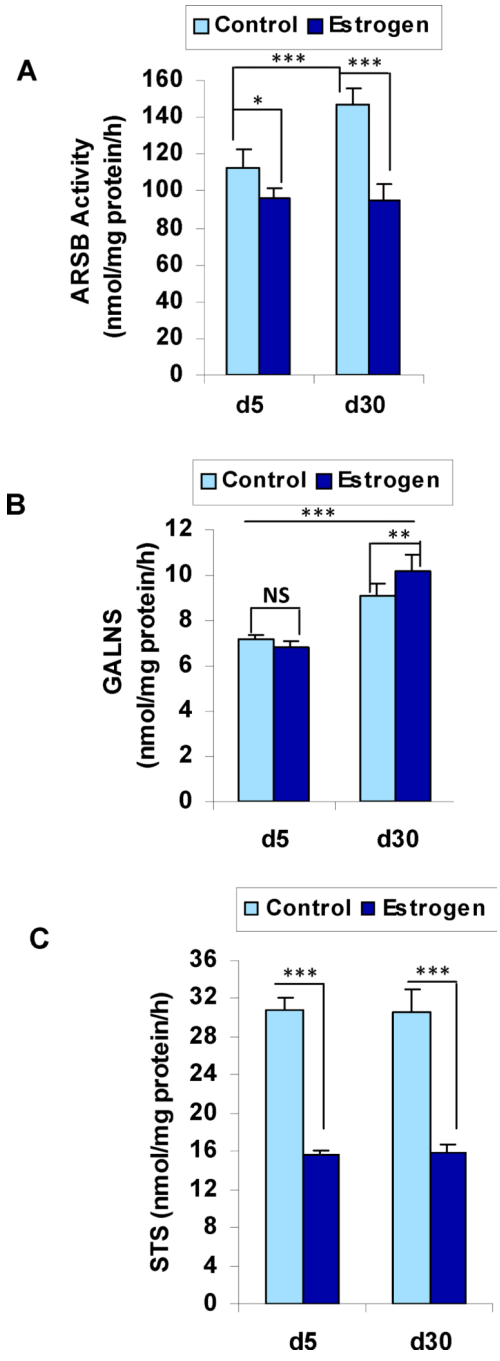

Figure 1. Sulfatase activity in rat prostate tissue on Days 5 and 30

A. ARSB activity increases between days 5 and 30 ($p<0.001$, one-way ANOVA with Tukey-Kramer post-test) in the oil control, but is significantly less in the estrogen-treated prostate tissue ($p<0.001$).

B. GALNS activity increases significantly between days 5 and 30 in both the control and estrogen-treated prostate tissue ($p<0.001$), and is significantly greater on day 30 following estrogen ($p<0.01$).

C. Steroid sulfatase activity is stable between days 5 and 30 for both control and estrogen-treated tissue, but is significantly less following exogenous estrogen ($p<0.001$).
[Statistical test is one-way ANOVA with Tukey-Kramer post-test. N for controls is 6 and for estrogen-treated is 6 for each time point. ARSB=arylsulfatase B; GALNS=Galactose-6-sulfatase; STS=steroid sulfatase]

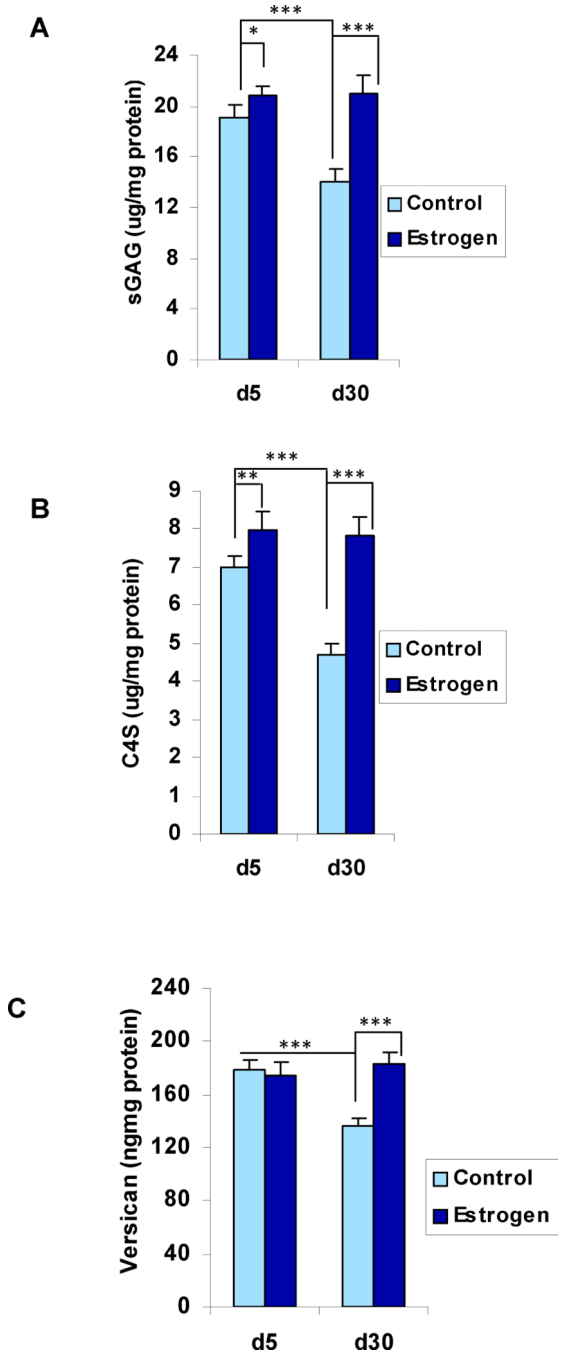

Figure 2. Total sulfated GAG, C4S, and versican in rat prostate tissue on Days 5 and 30

A. Total sulfated glycosaminoglycans decline between days 5 and 30 ($p<0.001$) in the control tissue, consistent with the increase in ARSB activity. With exogenous estrogen, total sGAG level is stable between days 5 and 30, reflecting both the inhibition of ARSB and the increase in GALNS between day 5 and day 30.

B. C4S decreases significantly in the control tissue between days 5 and 30 ($p<0.001$), consistent with the increase in ARSB activity. In the estrogen-treated tissue, the C4S is stable, consistent with the estrogen-induced inhibition of increase in ARSB activity.

C. Versican level declined between days 5 and 30 in the control ($p<0.001$), but this decline is inhibited by exogenous estrogen. The changes in versican are similar to those of total sulfated GAG and C4S.

[Statistical test is one-way ANOVA with Tukey-Kramer post-test. N=6 for controls, and N=6 for estrogen-treated at each time point. sGAG=sulfated glycosaminoglycan; C4S=chondroitin-4-sulfate; ARSB=arylsulfatase B; GALNS=Galactose-6-sulfatase]

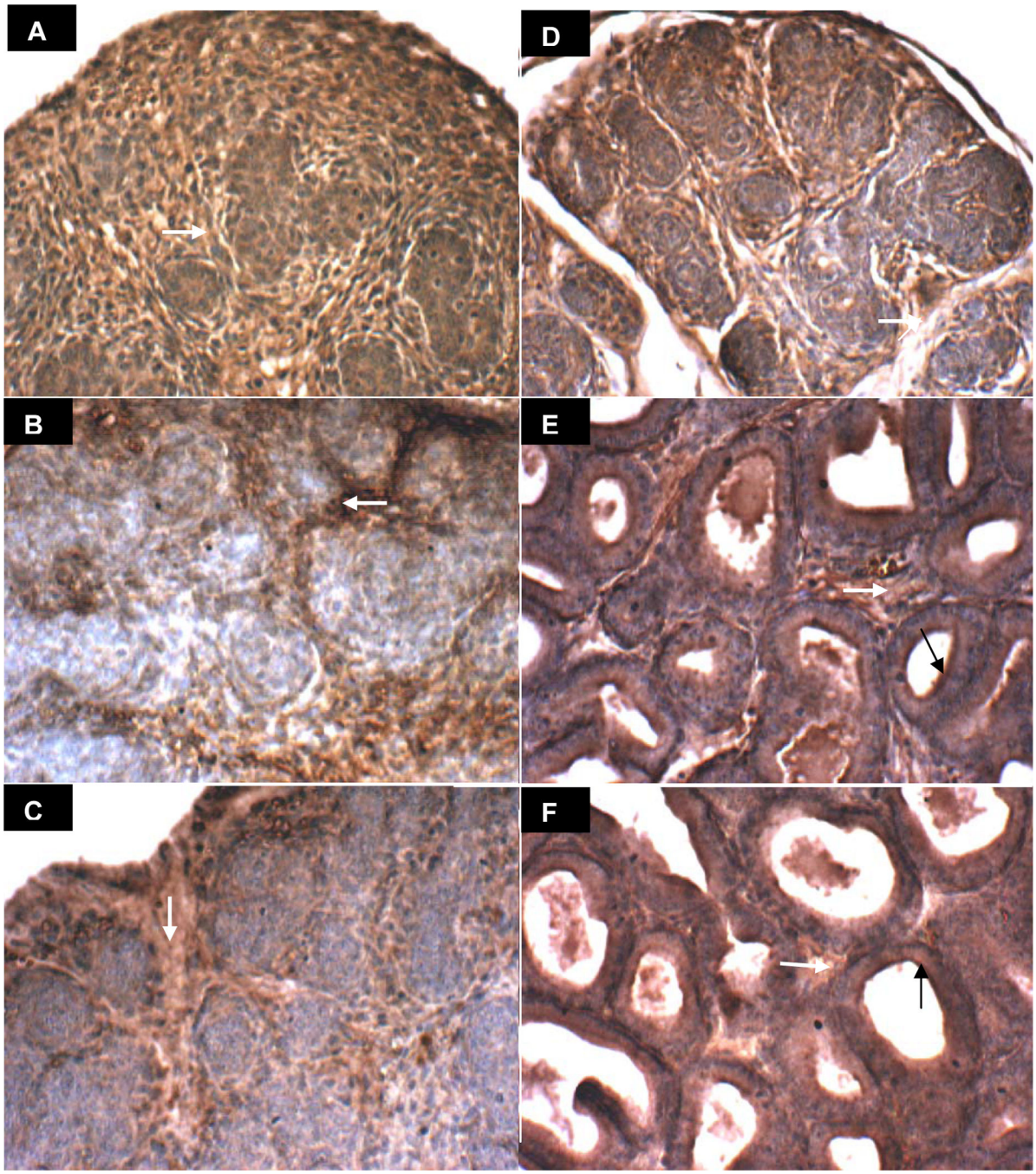

Figure 3. ARSB immunohistochemical staining of prostate tissue in oil control rats on Days 1–30

A-F. ARSB immunohistochemistry on days 1(**A**), 3(**B**), 6(**C**), 10(**D**), 15(**E**), and 30(**F**) demonstrates increasing definition of brown cytoplasmic immunostaining of ARSB in the stromal compartment, surrounding developing epithelial structures that do not stain at early time points. Negative ARSB epithelial staining is very well seen on days 3 and 6 (**B**), in which blue areas are prominent and are consistent with lack of epithelial ARSB. White arrows indicate representative sites of brown stromal immunostaining for ARSB. By days 15

and 30, ARSB is present at the luminal surface of epithelial cells (black arrows). [ARSB=Arylsulfatase B]

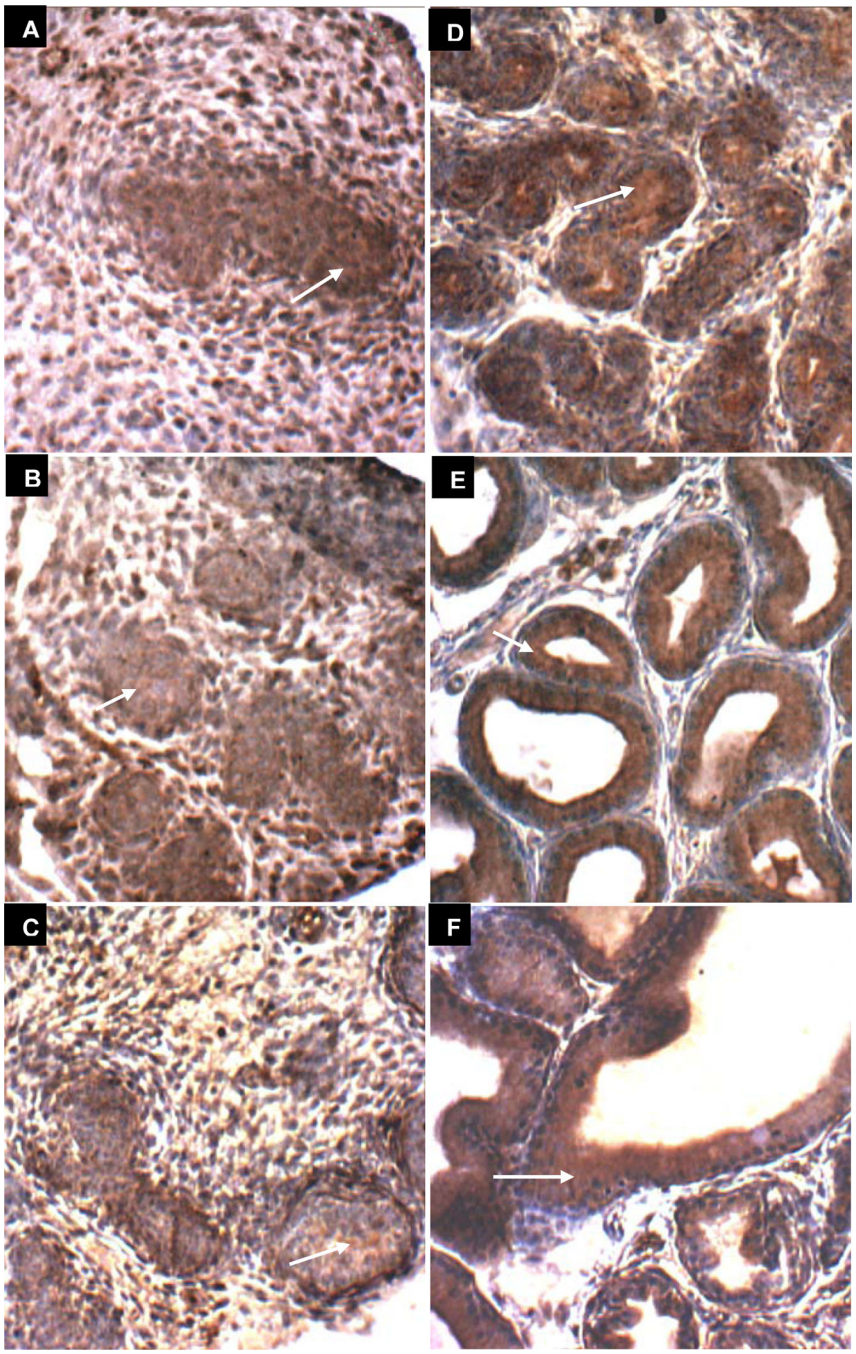

Figure 4. GALNS immunohistochemical staining of prostate tissue in oil control rats on Days 1–30

A-F. GALNS immunohistochemistry on days 1(**A**), 3(**B**), 6(**C**), 10(**D**), 15(**E**), and 30(**F**) demonstrates increasing definition of brown immunostaining of GALNS in the developing epithelial areas, surrounding an evolving lumen and distinct from the relatively non-staining (blue) stroma. White arrows denote representative sites of positive brown cytoplasmic staining of epithelial cells in developing acini. [GALNS=galactose-6-sulfatase]

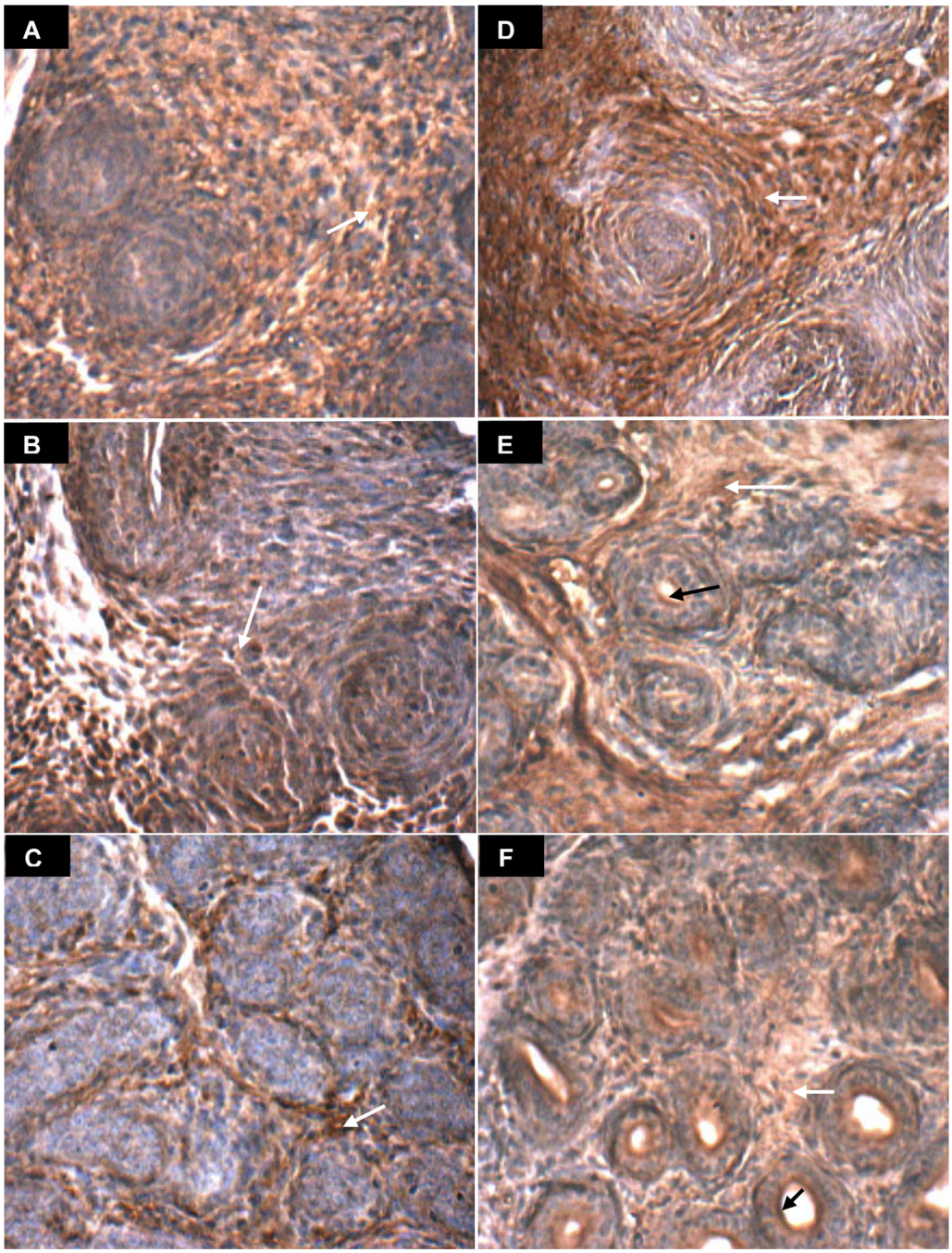

Figure 5. ARSB immunohistochemical staining of prostate tissue in estrogen-treated rats on Days 1–30

A-F. ARSB immunohistochemistry on days 1(**A**), 3(**B**), 6(**C**), 10(**D**), 15(**E**), and 30(**F**) following exogenous estrogen (estradiol benzoate 25 μg on days 1, 3, and 5) demonstrates prominent stromal immunostaining of ARSB (brown), surrounding the developing epithelial structures which are predominantly non-staining for ARSB and are blue. Overall staining intensity appears less than in the vehicle-only treated control (Fig. 3 A-F). Negative epithelial staining is prominent by day 6, in contrast to day 3 in the control, consistent with a

developmental delay. Luminal development at day 30 appears comparable to day 15 in the control. White arrows indicate representative stromal immunostaining for ARSB, which is less than in the vehicle control. Black arrows (**E, F**) indicate representative sites of prominent luminal epithelial cell membrane staining for ARSB [ARSB=Arylsulfatase B].

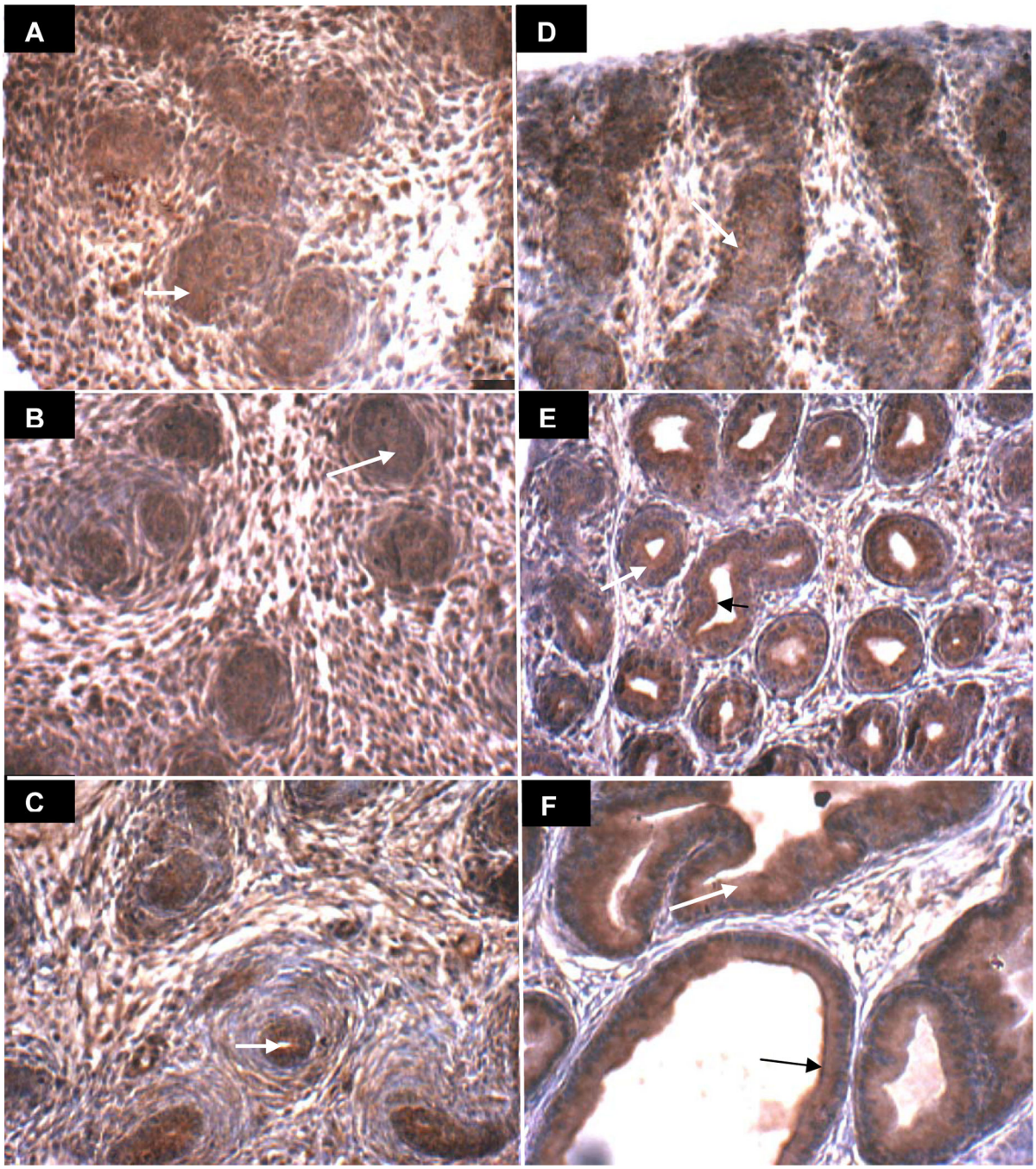

Figure 6. GALNS immunohistochemical staining of prostate tissue in estrogen-treated rats on Days 1–30

A-F. GALNS immunohistochemistry on days 1(**A**), 3(**B**), 6(**C**), 10(**D**), 15(**E**), and 30(**F**) following exogenous estrogen (estradiol benzoate 25 μg on days 1, 3, and 5) reveals increasing definition of the brown epithelial acinar structures surrounding a lumen and distinct from the relatively non-staining (blue) stromal regions. White arrows denote representative sites of brown epithelial cytoplasmic immunostaining for GALNS. Luminal

epithelial membrane appears to be positive for both ARSB and GALNS on days 15 and 30, indicated with black arrows. [GALNS=galactose-6-sulfatase]

Table 1

Sulfatase activity and total sulfated GAG, C4S, and versican on Days 5 and 30 in control and following exposure to estrogen

Measurement ± (S.D.) (n=6)	Day 5	Day 30	Day 5 + Estrogen	Day 30 + Estrogen
ARSB[a](nmol/mg protein/h)	112.4 (10.5)	146.5 (9.0) (***;###)[f,g]	96.1 (5.8) (*, NS)[h,i]	94.9 (8.4)
GALNS[b](nmol/mg protein/h)	7.2 (0.2)	9.1(0.5) (***, NS)	6.8 (0.3) (***,##)	10.2 (0.7)
STS[c] (nmol/mg protein/h)	30.7 (1.5)	30.6 (2.4) (NS,###)	15.6 (0.5) (NS,###)	15.8 (0.9)
C4S[d](μg/mg protein)	7.0 (0.3)	4.7 (0.3) (***,###)	8.0 (0.5) (NS,##)	7.8 (0.5)
Total sGAG[e] (μg/mg protein)	19.0 (1.0)	14 (1.0)(***,###)	20.8 (0.8) (NS, #)	20.9 (1.4)
Versican (ng/mg protein)	179.0 (7.5)	136.0 (5.5) (***,###)	179.4 (10.4) (NS,NS)	183.2 (7.9)

[a] ARSB = arylsulfatase B;

[b] GALNS = Galactose-6-sulfatase;

[c] STS = steroid sulfatase;

[d] C4S = chondroitin-4-sulfate;

[e] sGAG = sulfated glycosaminoglycans;

[f] control day 5 vs. control day 30;

[g] control day 30, vs. estrogen-treated day 30;

[h] estrogen=treated day 5 vs. estrogen treated day 30;

[i] estrogen-treated day 5 vs. control day 5;

***,### for p<0.001,

for p<0.01,

for p<0.05;

NS = not significant